



ELSEVIER

Computer Physics Communications 146 (2002) 30–37

Computer Physics
Communications

www.elsevier.com/locate/cpc

Carbon nanotube structures: molecular dynamics simulation at realistic limit

Maria Huhtala, Antti Kuronen, Kimmo Kaski *

Research Centre for Computational Science and Engineering, Helsinki University of Technology, P.O. Box 9400, FIN-02015 Hut, Finland

Abstract

Single walled carbon nanotubes as all-carbon molecules of tubular form exemplify modern nanometre scale material structures, where the number of atoms range from less than a million up to few millions. Such system are quite ideal for computational studies like Molecular Dynamics simulations because the studies can be done at the realistic limit, rendering them in a way predictive. This point of view we try to explore through simulations of novel ring-like carbon nanotubes, observed experimentally. Whether these structures are toroidal or coiled is under debate. To this question we seek insight by studying the structure, the minimum energy configuration, and the thermal stability of large toroidal nanotubes of (n, n) - and $(n, 0)$ -helicity using large scale Molecular Dynamics simulations based on the interaction potential by Brenner. The system sizes of the studied tori range one and half orders of magnitude, in diameter from about 22 nm up to 700 nm, where the latter corresponds to the sizes of experimentally observed ring-like structures. Our simulations indicate that the toroidal form influences strongly the structure of the tubes for small tori while for the larger tori the structural changes are extremely small. We also find that there exists a critical tube radius dependent buckling radius at which the torus buckles. This was also found to be helicity dependent. © 2002 Elsevier Science B.V. All rights reserved.

Keywords: Molecular dynamics; Carbon nanotube; Torus

1. Introduction

Recent development of microsystems has shrank them in many cases to nanometre scale showing in some cases novel material features. Over the past decade such a development is exemplified by the discovery [1] and then the vigorous research activity on carbon nanotubes. These tubular all-carbon molecules in their single walled form have the tube diameter ranging from as small as 0.4 nm to typically of a few nanometres and in length up to several microm-

eters. Thus the number of atoms these systems typically include ranges from less than a million up to few millions, which renders these systems quite ideal for studying some of their structural properties accurately with computational techniques like Molecular Dynamics simulation. Thus these studies can be done at the *realistic limit* and their accuracy depends on how well the interactions between atoms are described and on how long the simulations could be run. The former is dependent on the development of atomistic potentials and the latter on the development of computers and especially on computing methods and algorithms. These developments together with the fact that various modern material systems are shrinking to nanometre

* Corresponding author.

E-mail address: kimmo.kaski@hut.fi (K. Kaski).

scale are bound to make computational studies more and more *predictive*. Although it seems that such development would let us free from finite size considerations in the study of nanoscale material systems it does not do so from any other considerations of statistical physics.

With these in mind we focus here on studying some carbon nanotube structures. Although many of them seem to remain as pure speculation, Liu [2] and Martel et al. [3,4] have reported single walled carbon nanotubes and ropes of them forming ring-like structures, some of which suspected to be toroidal. Such toroidal structures are very interesting, for example because a nanotorus system has been theoretically shown to possess unusual electronic and magnetic properties like serving as a prototype for quantum wire ring [5,6].

Apart from some recent experimental studies of nanotori [2–4,7] very little is known about their structure, for example, how the torus curvature influences its local structure. In order to address this question we have performed large scale molecular dynamics simulations, which we also expect to give some insight to the structure of carbon nanotubes under uniform bending strain. In the previous numerical studies the systems have consisted of a few hundred, or at most a few thousand atoms [5,8–13]. In these very small systems the curvature of the structure is induced by locally adding pentagons and heptagons into the structure [8–12], or by combining nanotubes of different helicity [5,13]. However, in the experimental studies the diameters of the observed ring-like structures seemed to be much larger, typically between 300 and 500 nm [2,7] and 600 and 800 nm [3,4]. Theoretically this issue of torus diameter has been addressed by Meunier [6] from the elasticity theory point of view, suggesting that the curvature in large tori is more likely due to uniform bending than due to pentagon–heptagon defects. Apart from very small tori with (5, 5)-, (8, 8)-, and (10, 10)-helicity and diameter less than 60 nm studied by Han [14], to our knowledge nanotori of sizes equivalent to those experimentally observed have not been studied before with atomistic scale simulations. For this reason, and in order to shed more light to curvature generating mechanisms in nanotorus structures we have conducted large scale molecular dynamics simulations in systems with the number of atoms equivalent to the numbers in the experimentally observed structures.

This paper is organized as follows. Next we briefly introduce the molecular dynamics simulation method, with the choice of atomistic potential. With this model we first investigate minimum energy configurations of relaxed nanotube and nanotorus structures. Then we look in detail at the deformation in the cross section of a nanotorus as a function of the torus diameter. This is followed by a study of thermal stability of various torus structures. Finally, we draw conclusions.

2. Simulation method

In this work we have employed a classical molecular dynamics method, where the atomic interactions are described by the potential energy function of the form of a reactive empirical bond-order hydro-carbon potential formulated by Brenner [15]. This model was chosen because it has provided a good accuracy in the simulation of various carbon structures and because simulations with large system sizes are feasible with it. In comparison to another much used empirical potential energy model, namely Tersoff's model [16], the chosen model avoids the overbinding of radicals of which Tersoff's model suffers [15]. It should be noted that this formulation was originally developed for the study of chemical vapor deposition of diamond, but it has proven to be successful also in describing toroidal [10] and straight carbon nanotubes [18]. It is noted that Brenner's potential also reproduces the thermal properties of carbon accurately [19].

In this work we will use Brenner's first parameterization presented in Ref. [15], which has been found to provide a good description of bond-lengths but on the other hand yields too small stretching force constants. The second parameterization also provided by Brenner in Ref. [15] reproduces force constants that are in better agreement with experiment but with bond lengths seemingly too long. Since in the present study the torus structure is expected to be very little distorted for large tori, the first parameterization has been used. Because of the choice of the potential parameterization, the observed structural distortions might be enhanced slightly.

In order to find a relaxed minimum energy configuration for the tori, a reasonably fast relaxation method is required in the computations. For this we have chosen a gradient cooling method, in which the velocity

components of each particle are manipulated depending on the components of the gradient of the potential, the particle acceleration. In this method the directions of the components of the acceleration and the velocity of the particle are checked at each time step. If the components are in the same direction, the velocities are left intact but if they are in the opposite directions, the velocity is scaled down by a factor α . In practice, for each component a check whether $v_i \cdot a_i < 0$ is true is performed. The closer the value of α is to zero the faster the cooling process is but if the cooling is too fast, the particles get easily stuck into a local energy minimum. In the simulations we chose $\alpha = 0.8$ based on test runs and as a compromise between convergence speed and accuracy.

3. Minimum energy configuration

First we remind that in the characterization of nanotube structures the (n, m) -indexing is generally used. In this the circumference of a cut-open and unrolled tube is expressed by a vector that is a sum of integer multiples of two base vectors of a hexagonal 2D-lattice, i.e. $\vec{C} = n\vec{a}_1 + m\vec{a}_2$, for more details see Ref. [17]. In our study the initial atomic configurations of nanotubes were obtained by creating the planar hexagonal carbon atom network corresponding to an (n, m) -nanotube cut open axially. The nearest neighbor distances between carbon atoms were set to that of graphite, 1.421 Å. This plane was then mapped onto a 3D-cylindrical surface to form the tube and from this configuration the tube was further mapped to a torus as discussed next.

According to Meunier [6] and Han [14] the torus configuration in which strain is uniformly distributed is more stable for large toroidal structures than the configuration in which strain is localized to defects. This is supported by the experimental observations of Liu et al. [2] and Martel et al. [3], because the size of the observed rings is restricted to a well defined diameter range—the ring formation appears to be a thermally controlled process. Therefore, for our simulations we have chosen to generate the initial toroidal configurations by mapping the straight tube configuration in space so that the tube ends come next to each other to form a closed torus. The initial torus size is chosen such that the average of the inner and

outer diameters of the torus is the length of the tube forming the torus, if unbent. This quantity is also used to describe the torus size, i.e. the average of the inner and outer torus radii, or, in other words, the average particle distance from the center of mass of the torus.

Since in the study of the torus minimum energy configuration we will compare the toroidal nanotubes with relaxed straight tubes, some observations of the potential energy model of the unbent tubes will be discussed first. The minimum energy values of straight tubes were obtained by relaxing the initial tubular configuration both axially and radially while periodic boundary conditions were employed in the axial direction. The relaxation gives a difference of less than 0.2% for the relaxed tube length and for the initial regular hexagon based length. The change in the axial bond length is found to be largest for the tubes small in diameter. On the other hand the helicity seems to influence the sign of the change: relaxed configurations of the (n, n) -tubes are a little longer while the configurations of the $(n, 0)$ -tubes are a little shorter than the initial configurations. The difference is, however, very small. The change in the radial dimension from the regular hexagonal configuration is somewhat larger: for the smallest simulated tubes, that is, $(9, 0)$ - and $(5, 5)$ -tubes, the relaxed diameter is approximately 1% larger than the initial one and the change decreases to approximately 0.1% for the large tubes. This can be understood on the basis that a large curvature changes more the bond lengths from the regular hexagonal configuration of a graphene plane.

The toroidal structures that have been studied in this work are of (n, n) - and $(n, 0)$ -helicity and have diameters of approximately 22, 220, and 700 nm, where the largest size corresponds to what has been found in the experimental studies [2–4,7]. These torus sizes correspond to tube lengths of 0.07, 0.7, and 2.2 μm and the number of atoms in the simulations ranges from 5680 to 412960. For the study of the torus structure and its minimum energy configuration the toroidal initial configurations were relaxed using the gradient cooling method. In the beginning of the simulations the velocities of the particles were set random both in magnitude and in direction, in such a way that the distribution obeyed the Maxwell–Boltzmann distribution. The initial temperature of the system was set to 100 K.

In Fig. 1 we present the potential energy values per particle for the relaxed toroidal structures. The figure shows that there is very little helicity dependence in the bonding energy of the tori. The tube diameters have been defined by determining the center of mass axis of an unbent relaxed tube and calculating the average distance of the mass points representing the atoms to the axis. In other words, if the values are compared with experimental ones, the thickness of the nanotube wall must be added.

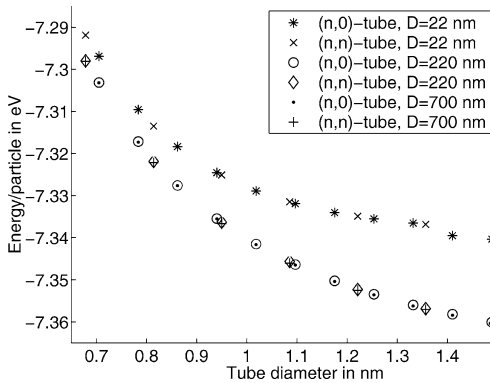


Fig. 1. Potential energy curve of relaxed toroidal structures as function of tube diameter for different torus diameters D . At about 1.35 nm tube diameter there appears a small kink for tori 22 nm in diameter.

A small kink can be distinguished in Fig. 1 in the potential energy for the tori with a diameter of 22 nm. This kink in the potential energies corresponds to a structural change in the minimum energy configuration of the torus due to the fact of becoming buckled, as demonstrated in Fig. 2. In this set of figures the length of the tube forming the torus is unchanged, i.e. 70 nm, but the tube radius changes increasing from Fig. 2(a) to Fig. 2(d) and from Fig. 2(e) to Fig. 2(h). The observed buckling pattern, meaning the number and the size of the buckles, depends on both the torus and the tube radius but also on the initial velocity distribution and on the cooling method. This can be observed close to the buckling radius, where the structures of Fig. 2 seem to exhibit some periodicity. Using a different seed value for the random number generator in setting up the initial velocity distribution of the atoms or starting from a different initial temperature results in a different buckling pattern. The configurations shown in Fig. 2 correspond to only one energy minimum amongst many minima close to each other in energy.

The critical buckling diameter of a torus was studied also by varying the tube length, i.e. torus diameter, instead of the tube diameter. Fig. 3 shows the results. Also in this case there is a kink in the potential energy at the critical buckling radius. The results are in excellent agreement with the ones reported by Han [14]. In our calculations an (8, 8)-torus seemed to

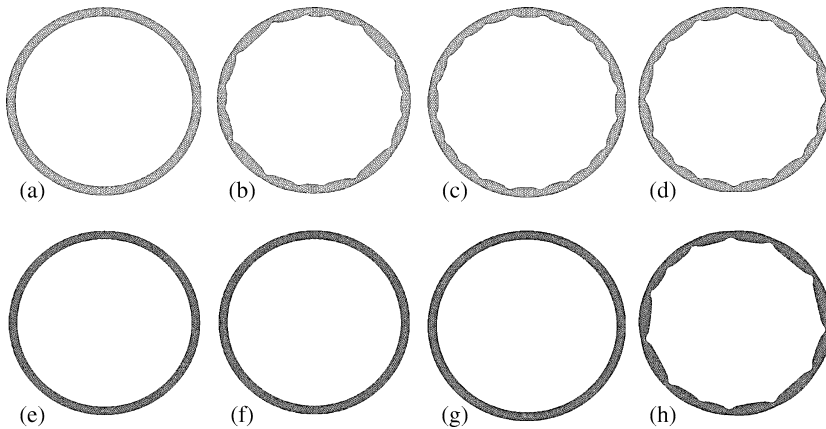


Fig. 2. Minimum energy configurations of nanotori 22 nm in diameter for different tube diameters d . (a) (17, 0)-tube, $d = 1.33517$ nm; (b) (18, 0), 1.41328 nm; (c) (19, 0), 1.49130 nm; (d) (20, 0), 1.56938 nm; (e) (8, 8), 1.08789 nm; (f) (9, 9), 1.22300 nm; (g) (10, 10), 1.35828 nm; (h) (11, 11), 1.49344 nm. When the tube diameter d increases a structural change is observed. The onset of buckling appears as a small kink in the potential energy curve of Fig. 1.

buckle at a diameter of approximately 13 nm, which is to be compared with the buckling diameter value being between 8 and 16 nm reported by Han. It should also be noted that in our studies the tubes were chosen so that the radius of an $(n, 0)$ - and the corresponding (n, n) -tube match as well as possible. This enables us to see if helicity influences the buckling. The results indicate that the critical buckling diameter is smaller for the (n, n) -torus than for the $(n, 0)$ -torus with the same tube diameter.

In order to find out how the strain is distributed in the buckled torus we have computed the potential energy distribution. As expected the strain was found to

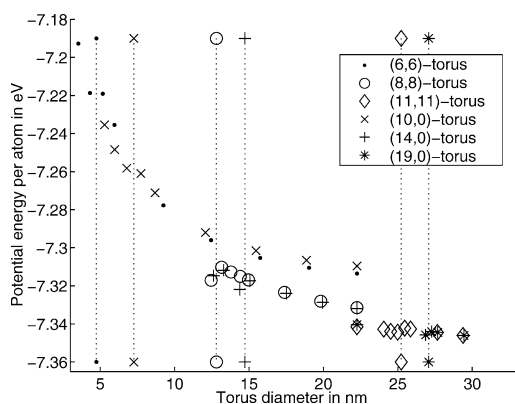


Fig. 3. Critical buckling diameter of (6, 6)-, (8, 8)-, (11, 11)-, (10, 0)-, (14, 0)-, and (19, 0)-tori. The buckling radius is marked by a vertical dotted line marked by the symbol representing the tube.

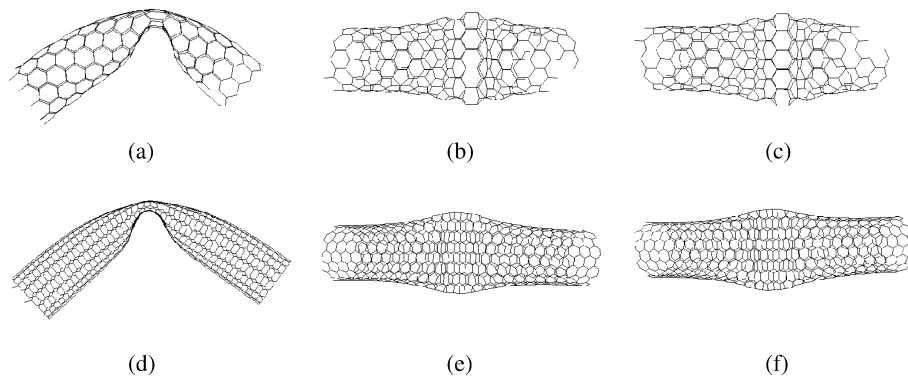


Fig. 4. Sample bends in buckled nanotori of a (10, 0)-torus with 1560 atoms ((a)–(c), side, inside and outside views, respectively) and similarly an (8, 8)-torus with 4608 atoms ((d)–(f)). The hexagonal bonding configuration is deformed but otherwise intact. The images of the (10, 0)- and the (8, 8)-tube sections are not in the same scale because of different diameters.

be localized to the folding corners, which raises the question, whether the hexagonal bonding configuration is still maintained or whether bond reorganization has taken place. Fig. 4 shows samples of a (10, 0)-torus and an (8, 8)-torus with buckling. In these samples it is seen that the hexagonal bonding configuration is deformed but no actual bond breakage has occurred. However, if the torus size is decreased, eventually bond breakages will take place as the strain becomes larger. Previous studies have indicated that it is energetically favorable for the curvature in tori this small to be induced by creating pentagons and heptagons [14]. Then a question arises why have we not observed them in our simulations. The answer lies in the formation energy barrier of defects such that there is not enough kinetic energy for the defects to be formed as the initial configuration does not contain them. We have looked into this by exposing a torus to a heat bath and found that thermal energy enables bond reorganization and strain relaxing defect formation, especially combinations of pentagon–heptagon pairs. This issue we will investigate in more detail in the future.

4. Cross section deformation

Now we will discuss how the bending of a tube to a toroidal form deforms the tubular cross-section. In the study by Han [14] the quantitative behavior of (5, 5)-, (8, 8)-, and (10, 10)-tori of a diameter less than 60 nm was discussed. There the bending strain was found

to deform the tubular cross-section to an ellipsoidal shape with the major axis perpendicular to the plane of the torus. It was also reported that if the strain was large enough, the tube was found to buckle and for still larger strain values bond breakages were found to occur. Here we will discuss these issues in more detail and for a larger variety of tubes of both (n, n) - and $(n, 0)$ -helicity. We have studied torus deformation under various bending conditions systematically as a function of the tube diameter for tori of three different diameters: 22, 220, and 700 nm.

We have calculated the amount of cross-sectional deformation by first defining the center of mass for the relaxed torus. To do this the torus was divided into N equal sectors, where the value of N was defined so that each sector consisted of a little over one unit cell of an unbent tube. The amount of atoms in a unit cell for tubes of both (n, n) - and $(n, 0)$ -helicity is $4n$ [17]. Therefore values of $N = 540$, $N = 5000$, and $N = 16000$ were used for the (n, n) -tubes and correspondingly $N = 270$, $N = 2500$, and $N = 8000$ for the $(n, 0)$ -tubes. In each sector the atom with the largest and the atom with the smallest radial distance from the center of mass were searched, to represent the outer and the inner radius of the torus in that sector, respectively. Their difference represents the radial cross section diameter. The non-radial cross section diameter in each sector was defined as the distance between the atoms that were furthest from the plane of the torus. Then the average over the sectors was used as the characteristic value for the whole torus. This method is expected to give a good estimate for the diameter because of the regular carbon nanotube structure and because we have not seen any bond breakages or stray particles in the simulations.

As a further analysis of this method we calculated the standard deviations for the radial and non-radial cross section diameters over the different sectors of the tori to serve as a measure of how symmetrical the atomic configurations are and how well the method is able to define the diameters. We also varied the values of N and observed that the above N values were seen to be justified because the standard deviation for them was minimized. The structures, except for the buckled configurations of Fig. 2, are highly symmetrical and standard deviation of the defined diameters is very small, of the order 10^{-2} .

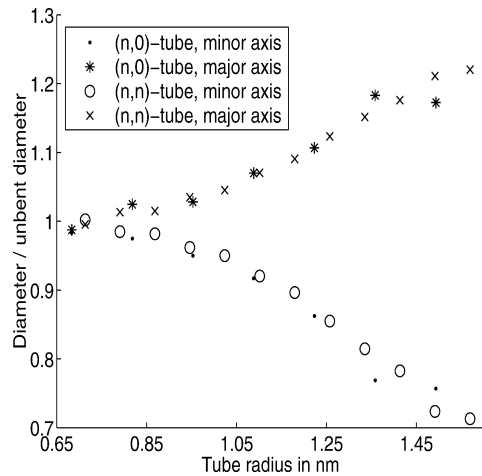


Fig. 5. Relative tubular cross section deformation of nanotubes bent into a torus 22 nm in diameter.

In Fig. 5 we present the relative tubular cross section diameter values for the tori 22 nm in diameter. This figure shows that the tubular cross section can deform as much as 20% before buckling occurs. The helicity of the tube structure was not found to influence the cross sectional deformation significantly. The analysis of this deformation in the case of large tori showed that it is very small, in fact less than 0.1% for the tori with diameter of 220 nm and seem to vanishes completely for the tori 700 nm in diameter.

5. Thermal stability

Now we move on to look at the thermal stability of these nanotori. This we have done quite coarsely by simulating the time development of the minimum energy configurations of atoms of the torus at a finite temperature. The initial velocities of the atoms were set at random following the Maxwell–Boltzmann distribution. The average system temperature was first kept at the chosen value for 300 fs, that is, 300 simulation time steps, by scaling the atomic velocities after each time step. After that the system was let to evolve free of constraints for 3000 fs.

Using this approach we have observed that although the interaction model used in this work reproduces thermal properties of carbon nanotubes relatively well [19], it predicts a somewhat higher melting

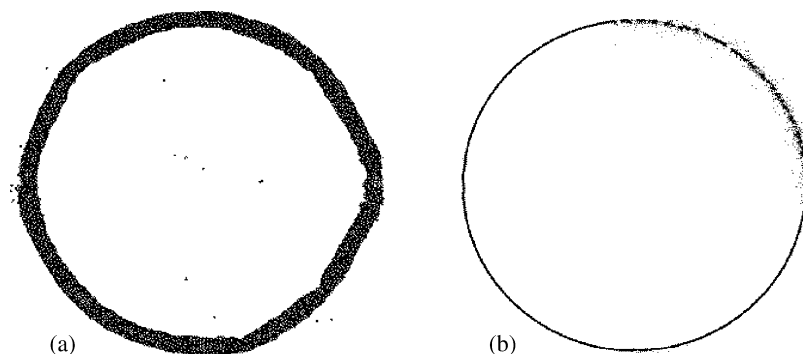


Fig. 6. Two (8, 8)-tori with different diameters simulated for 3000 fs at different temperatures. (a) $D = 22$ nm, $T = 1500$ K; (b) $D = 220$ nm, $T = 5500$ K. In (a) bond breakages can be seen but the structure remains toroidal. If the temperature is raised more, the toroidal structure breaks apart. In (b) bond breakages have evolved further and a part of the torus has already dissolved.

temperature than observed experimentally. Similar observations are reported also in Ref. [19]. The melting temperatures for the large tori turned out to be higher than experimentally observed for bulk graphite even though the extra strain due to curvature should decrease the melting temperature. In addition we have found that the tube diameter influences the melting temperature much more than the torus diameter would do. For the tori 22 nm in diameter and made of nanotubes very small in diameter, the toroidal form maintains up to the temperature of 1000 K, whereas the tori formed of larger tubes with tube diameters ranging between 1.1 and 1.6 nm hold up to almost the temperatures of the larger tori. Despite the fact that the potential energy curves of the tori show a downward kink at the buckling radius, the buckled tori are thermally less stable than the ones with an elliptical cross section. This is due to the local, unevenly distributed buckling strain. Large tori hold their form up to the simulation temperature of approximately 5000 K depending on the tube radius. There does not seem to be any significant difference between the results of the tori 220 nm in diameter and of the tori 700 nm in diameter. In Fig. 6 we show two images of tori simulated at high temperatures. The given temperature values are averages, as can be seen in Fig. 6(b), where the temperature is distributed unevenly and is higher in the dissolved section than in the other parts of the torus.

In these finite temperature simulations we have also observed that there appears a some sort of strong collective motion behaviour in the tori. This behavior of the torus circumference resembles of a snake that

has eaten something too large—thinner and larger lumps seem to propagate along the circumference. When these lumps become too large, bond breakages start to occur and the torus start to evaporate. Such a collective motion behavior is either an inherent property of carbon nanotori or it is a feature arising from the use of the minimum energy configuration as the initial configuration. In the latter case the coupling with a heat bath could cause thermal expansion in the structure and induce collective motion.

6. Conclusions

Large toroidal carbon nanotubes were studied using molecular dynamics simulations. Our studies indicate that the experimentally observed rings are thermally stable and that the curvature does not cause significant structural changes in the tori with the size similar to those observed experimentally [2–4,7]. For tori significantly smaller than that the cross section was found to deform elliptically, before reaching a critical radius, below which, the torus was found to buckle. This buckling does not change the hexagonal bonding configuration although the bonding angles change to account for the buckles.

Nanotori of (n, n) -helicity seem to have a smaller buckling radius than the corresponding tori of $(n, 0)$ -helicity. This may have important consequences from the point of view of applications. Buckling induces more drastic changes in the conductivity properties than an elliptical deformation and therefore a differ-

ence in the buckling radius is significant for those electronics applications in which uniform bending strain can be expected.

These results and the discussion can be extended to bent nanotubes, because such structures could be under similar local strain conditions as the toroidal structures. Experimental observations of nanotube bends [20,21] seem to show similar buckling behavior as we report here.

References

- [1] S. Iijima, *Nature* 354 (1991) 56.
- [2] J. Liu, H. Dai, J.H. Hafner, D.T. Colbert, R.E. Smalley, S.J. Tans, C. Dekker, *Nature* 385 (1997) 780.
- [3] R. Martel, H.R. Shea, P. Avouris, *Nature* 398 (1999) 299.
- [4] R. Martel, H.R. Shea, P. Avouris, *J. Phys. Chem. B* 103 (1999) 7551.
- [5] R.C. Haddon, *Nature* 388 (1997) 31.
- [6] V. Meunier, P. Lambin, A.A. Lucas, *Phys. Rev. B* 57 (1998) 14886.
- [7] M. Ahlskog, E. Seynaeve, R.J.M. Vullers, C. van Haesendonck, A. Fonseca, K. Hernadi, J.B. Nagy, *Chem. Phys. Lett.* 300 (1999) 202.
- [8] B.I. Dunlap, *Phys. Rev. B* 46 (1992) 1933.
- [9] S. Itoh, S. Ihara, J. Kitakami, *Phys. Rev. B* 47 (1993) 1703; S. Ihara, S. Itoh, J. Kitakami, *Phys. Rev. B* 47 (1993) 12908; S. Itoh, S. Ihara, J. Kitakami, *Phys. Rev. B* 48 (1993) 5643; S. Itoh, S. Ihara, *Phys. Rev. B* 48 (1993) 8323; S. Itoh, S. Ihara, *Phys. Rev. B* 49 (1994) 13970.
- [10] J.K. Johnson, B.N. Davidson, M.R. Pederson, J.Q. Broughton, *Phys. Rev. B* 50 (1994) 17575.
- [11] R. Setton, N. Setton, *Carbon* 35 (1997) 497.
- [12] H. Terrones, M. Terrones, *Carbon* 36 (1998) 725.
- [13] D. Oh, J.M. Park, K.S. Kim, *Phys. Rev. B* 62 (2000) 1600.
- [14] J. Han, *Chem. Phys. Lett.* 282 (1998) 187.
- [15] D.W. Brenner, *Phys. Rev. B* 42 (1990) 9458; D.W. Brenner, *Phys. Rev. B* 46 (1992) 1948.
- [16] J. Tersoff, *Phys. Rev. Lett.* 56 (1986) 632; J. Tersoff, *Phys. Rev. B* 37 (1988) 6991; J. Tersoff, *Phys. Rev. B* 39 (1989) 5566.
- [17] R. Saito, G. Dresselhaus, M.S. Dresselhaus, *Physical Properties of Carbon Nanotubes*, Imperial College Press, 1998.
- [18] B.I. Yakobson, C.J. Brabec, J. Bernholc, *Phys. Rev. Lett.* 76 (1996) 2511; C.F. Cornwell, L.T. Wille, *J. Chem. Phys.* 109 (1998) 763; M.B. Nardelli, B.I. Yakobson, J. Bernholc, *Phys. Rev. Lett.* 81 (1998) 4656; M.B. Nardelli, B.I. Yakobson, J. Bernholc, *Phys. Rev. B* 57 (1998) 4277; A. Garg, S.B. Sinnott, *Phys. Rev. B* 60 (1999) 13786.
- [19] J.N. Glossli, F.H. Ree, *J. Chem. Phys.* 110 (1999) 441.
- [20] M.R. Falvo, G.J. Clary, R.M. Taylor II, V. Chi, F.P. Brooks Jr., S. Washburn, R. Superfine, *Nature* 389 (1997) 582.
- [21] O. Lourie, D.M. Cox, H.D. Wagner, *Phys. Rev. Lett.* 81 (1998) 1638.